Technical Annals

Vol 1, No 9 (2025)

Technical Annals

Seismic Protection of Onshore Wind Turbines using Novel Vibration Control Systems

Konstantinos Kapasakalis, Georgios Florakis, Evangelos Sapountzakis

doi: 10.12681/ta.40478

To cite this article:

Kapasakalis, K., Georgios Florakis, & Evangelos Sapountzakis. (2025). Seismic Protection of Onshore Wind Turbines using Novel Vibration Control Systems. *Technical Annals*, *1*(9). https://doi.org/10.12681/ta.40478

Seismic Protection of Onshore Wind Turbines using Novel Vibration Control Systems

Konstantinos Kapasakalis[1[0000-0002-6619-7374]], Georgios Florakis[1[0000-0003-3061-1542]] and Evangelos Sapountzakis[1[0000-0002-1677-3070]]

[1]Institute of Structural Analysis and Antiseismic Research, School of Civil Engineering, National Technical University of Athens, Zografou Campus, GR-157 80 Athens, Greece
kapasakalis@central.ntua.gr, giorgosfls@mail.ntua.gr, cvsapoun@central.ntua.gr

Abstract. As the climate crisis intensifies, the transition to renewable energy sources has become more critical than ever, with wind energy playing a key role in reducing carbon emissions and ensuring a sustainable future. To maintain the reliability of wind power infrastructure, it is essential to enhance the structural resilience of wind turbines (WT). In seismic prone regions, earthquakes can generate forces that exceed the structural strength of WT towers, leading to potential failures. This study addresses this challenge by proposing novel vibration control systems to seismically protect WT structures, ensuring stability and continued operation of wind energy infrastructure. In this paper, various vibration control systems (VCS) are implemented in a benchmark onshore wind turbine tower to enhance its seismic resilience against severe earthquakes. The employed VCS are based on the KDamper concept, an extension of the traditional Tuned Mass Damper (TMD) with the strategic introduction of negative stiffness and damping elements. The VCS are designed using a constrained optimization methodology with ground motion acceleration input based on EC8 provisions. For comparison, a TMD with 20 times higher additional mass is also evaluated. Numerical results demonstrate that the KDamper-based designs outperform the classical TMD, offering a viable solution for seismic protection of onshore WT.

Keywords: Wind Turbine Structures, Seismic Protection, Vibration Control Systems, Negative Stiffness, Damping.

1 Introduction

In recent decades, the installation of both offshore and onshore wind turbines (WTs) has increased rapidly due to the growing demand for renewable energy. Large rotors and taller, slender towers have emerged as the prevailing design for modern turbines, facilitating higher power output but also introducing additional structural challenges associated with the increased gravitational and rotational loads. Furthermore, wind turbines are subjected to complex loading scenarios, including aerodynamic forces from wind gusts, seismic forces in regions of moderate-to-high seismicity and in the case of offshore wind turbines (OWTs), hydrodynamic forces from waves, currents and tidal

effects. These loads not only compromise the turbines' contribution to the energy network but also induce excessive structural vibrations and fatigue in their towers, potentially leading to structural failure [1, 2]. Hence, mitigating excessive vibrations remains a top priority in the design and operation of these structures.

Numerous vibration control systems (VCS) have been introduced to safeguard both structures such as offshore and onshore WTs. These systems can be broadly categorized as passive [3-6], active [7, 8], hybrid [9], or semi-active [10, 11, 12], with passive solutions being the most common in engineering applications [13-15] due to their relative simplicity, cost-effectiveness and reliability. Among passive systems, Tuned Mass Dampers (TMDs) have garnered particular interest in the WT vibration mitigation literature [3,5]. A standard TMD consists of a secondary mass connected to the primary structure through a positive stiffness element and an artificial damper. In wind turbines, it is typically placed near the top of the tower or inside the nacelle to take advantage of the high amplitude of motion at these locations. By tuning the TMD's frequency to coincide with a primary mode of vibration, a significant portion of the turbine's vibratory energy can be diverted and dissipated by the secondary mass. The implementation of two independent TMDs within the nacelle has also been proposed in [4] to effectively mitigate both fore-aft and side-to-side modal responses. Furthermore, the strategic placement of multiple TMDs along the tower of OWTs has been investigated in [16], as a means to control structural vibrations induced by the combined effects of multiple hazards, such as wind loads, sea wave forces and seismic excitations.

In an effort to enhance the protection of WTs against the various loading scenarios, modifications to TMDs have also been explored. The Pendulum Tuned Mass Damper (PTMD) [17], as its name suggests, is a TMD configuration in which the stiffness element is implemented using a pendulum. This device has proved to be highly effective in controlling and reducing structural vibrations in WTs caused by wind loads and low-to-medium intensity seismic excitations [18]. The Tuned Liquid Column Damper (TLCD) [19] is a U-shaped vibration control device that utilizes the movement of a liquid mass within a tubular container to counteract external forces, while an embedded orifice generates damping forces that facilitate energy dissipation. The integration of TLCDs in OWTs is anticipated to reduce structural vibrations and bending moments, thereby enhancing the fatigue life of the system [20, 21]. Additionally, alternative passive control strategies, such as the Ball Vibration Absorber (BVA) [22], the tuned rolling-ball damper [23] and the spherical tuned liquid damper [24] have been proposed for the vibration control of WT structures. The findings of these studies consistently demonstrate that passive control methods are effective in mitigating the undesirable vibrations in WT towers.

Despite their advantages, TMD-based systems have inherent drawbacks when applied to wind turbines. Foremost, effective TMD operation typically requires a large secondary (additional) mass placed often in or near the nacelle where the structural vibrations are most pronounced. However, this placement may be impractical due to space limitations, as the nacelle hosts critical mechanical and electrical components. Additionally, adding more mass elevates the tower's center of gravity and increases the axial force, heightening the risk of higher-order dynamic phenomena, particularly in highly flexible, tall WT towers. Furthermore, TMDs are parameter sensitive [25],

meaning even minor deviations in tuning frequency or damping values can lead to diminished performance. Such tuning errors may result from manufacturing inaccuracies, unmodeled structural nonlinearities, variations in operating conditions or temperature fluctuations.

An emerging alternative to conventional TMDs is the KDamper concept as introduced in [26]. The KDamper extends the TMD configuration, amplifying indirectly the beneficial inertial effect of the secondary mass. This is achieved by incorporating a negative stiffness (NS) element into the device. Since the NS force is in phase with the inertial force of the secondary mass, the vibration absorption capacity can be significantly enhanced by adjusting the NS properties. Thus, the primary drawback of the TMDs, which is the need for a large moving mass to achieve effective vibration mitigation, is overcome with the KDamper concept. Notably, although the NS element reverses the usual direction of the stiffness force, the overall device remains both statically and dynamically stable within its range of motion, unlike other NS isolators such as Quasi-Zero-Stiffness (QZS) oscillators [27]. Additionally, the KDamper more effectively controls the tuning of its parameters and provides vibration attenuation across a broader frequency range compared to conventional TMD devices.

Several variations of the KDamper device have been proposed in the literature, namely the Extended KDamper (EKD) [28], the Seismic Base Absorber (SBA) [29] and the Enhanced KDamper (ENKD) [30]. The SBA and ENKD incorporate inerter elements [31] into their configurations. These three modifications, referred to as KDamper-based devices, further enhance the original device's performance in vibration control, effectively managing induced structural displacements and accelerations. Their effectiveness results from proper optimization [32, 33] and precise mechanical design [34, 35], with particular emphasis given to their NS mechanisms [36]. The KDamper-based devices have been extensively researched for a wide range of applications, including the horizontal protection of buildings [30, 32, 33, 37, 38, 39], vertical seismic absorption [40, 41] and vibration isolation in both bridges [42] and wind turbine towers [43, 44].

In this paper, the seismic protection of onshore wind turbines (WT) is investigated through the implementation of novel vibration control systems (VCS). The study focuses on the KDamper concept, an advanced extension of the traditional Tuned Mass Damper (TMD), which strategically incorporates negative stiffness and damping elements to enhance its vibration absorption capabilities. A benchmark WT tower is analyzed using a dynamic model formulated with prismatic beam elements, and numerical simulations are conducted using a custom-built MATLAB code. The VCS are designed through a constrained optimization methodology that accounts for engineering, manufacturing, and geometrical constraints and limitations, with seismic excitation input selected based on EC8 provisions by generating a database of artificial accelerograms compatible to the EC8 design acceleration spectrum. Comparative analysis against a conventional TMD with significantly higher additional mass (20 times) highlights the superior performance of the KDamper-based designs. The numerical results demonstrate that the proposed approach significantly improves the WT tower seismic resilience, reducing structural demands and ensuring greater stability of WT infrastructure against severe earthquake events.

2 Dynamic Model of Onshore Wind Turbine

The NREL 5-*MW* baseline three-bladed horizontal axis onshore wind turbine (WT) of 120*m* tower length and variable tubular cross-section $A_{WT}(x)$ [45] is examined in this paper and is presented in Fig. 1, along with the investigated vibration control systems (VCS) implemented for seismic protection. The WT tower base diameter is 8.43*m* with steel thickness 4.8*cm*, the top diameter is 3.87*m* with thickness 2.5*cm*, the Young's modulus is 210*GPa*, while the steel density is assumed to be equal to 8.5tn/m^3. To account for the inertial forces applied by the mechanical parts (nacelle, rotor and blades), an additional concentrated mass m_{NAC} = 403.22*tn* [45] is added at the top of the WT tower, as illustrated in Fig. 1.

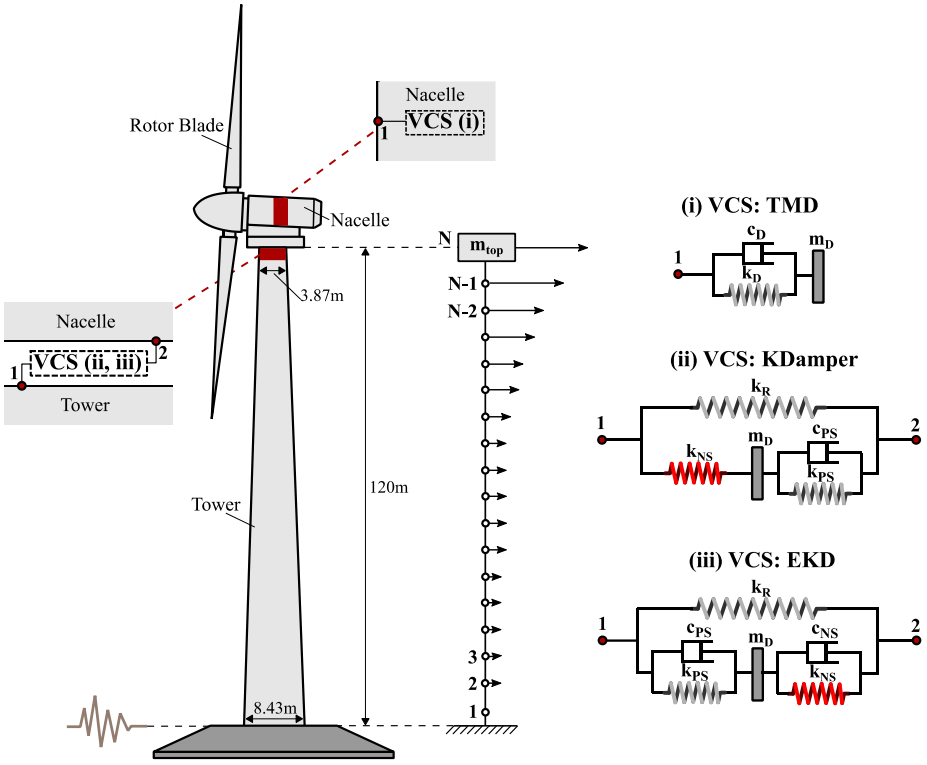

Fig. 1. Schematic representation of the onshore wind turbine tower with the investigated vibration control systems (VCS) implemented for seismic protection (TMD, KDamper, EKD), along with the lumped mass model for the WT tower.

The developed dynamic model of the WT tower is an assemblage of prismatic beam elements, i.e. the cross-sectional dimension within the elements remains the same. The dynamic degrees of freedom (DoFs) are the sway ones, while the rotational ones are condensed. Further assumptions made for the modelling are: a) the WT tower is considered to remain elastic under the dynamic loads (wind and seismic), b) the effects of

soil-structure-interaction are not accounted for (fixed base assumption), and c) the prismatic beam elements are inextensible, and thus the axial DoFs are not considered in this study. For the numerical modelling of the proposed formulation a built-in house software is developed in MATLAB code employing the Newmark-β method for the dynamic analysis.

The equations of motion of the onshore WT expressed in a matrix form are:

$$[M_{WT}]\{\ddot{u}_{WT}\} + [C_{WT}]\{\dot{u}_{WT}\} + [K_{WT}]\{u_{WT}\} = -[M_{WT}][I]\ddot{X}_G(t) + [W(t)] \quad (1)$$

where $[M_{WT}]$, $[C_{WT}]$ and $[K_{WT}]$ are the mass, damping and stiffness matrices of the original WT tower, respectively of order ($N \times N$), N indicating the number of prismatic beam elements selected to model the WT tower. The damping matrix $[C_{WT}]_{NxN}$ is not explicitly known but is obtained with the help of Rayleigh's approach using the same damping ratio in all modes, 1% [45]. The unknown nodal displacements$\{u_{WT}\}$, relative to the fixed base of the WT tower, are collected in the array $\{u_{WT}\} = \{u_1,u_2,u_3,\ldots,u_N\}^T$. In this research work 24 prismatic beam elements are used for the modelling of the onshore WT tower (N=24).

2.1 Proposed Vibration Control Systems

In Fig. 1 the proposed Vibration Control Systems (VCS) installed in the onshore WT for seismic protection are presented. The governing equations of motion of the controlled WT presented in a matrix form are the following:

$$[M]\{\ddot{u}\} + [C]\{\dot{u}\} + [K]\{u\} = -[M][I]\ddot{X}_G(t) + [W(t)] \quad (2)$$

where $[M]$, $[C]$ and $[K]$ are the mass, damping and stiffness matrices of the controlled WT tower, respectively having dimensions (N+n) x (N+n), n indicating the extra DoFs of each of the VCS to be considered. Furthermore, $\{u\} = \{\{u_N\}, \{u_n\}\}^T$ are the unknown, relative to the base displacements. A general formulation of the controlled system's matrices $[M]$, $[C]$ and $[K]$ is the following:

$$[M]_{(N+n)\times(N+n)} = \begin{bmatrix}[M_{WT}]_{N\times N} & [0]_{N\times n}\\ [0]_{n\times N} & [0]_{n\times n}\end{bmatrix} + \begin{bmatrix}[M_{WT-WT}]_{N\times N} & [M_{WT-VCS}]_{N\times n}\\ [M_{VCS-WT}]_{n\times N} & [M_{VCS-VCS}]_{n\times n}\end{bmatrix} \quad (3.1)$$

$$[K]_{(N+n)\times(N+n)} = \begin{bmatrix}[K_{WT}]_{N\times N} & [0]_{N\times n}\\ [0]_{n\times N} & [0]_{n\times n}\end{bmatrix} + \begin{bmatrix}[K_{WT-WT}]_{N\times N} & [K_{WT-VCS}]_{N\times n}\\ [K_{VCS-WT}]_{n\times N} & [K_{VCS-VCS}]_{n\times n}\end{bmatrix} \quad (3.2)$$

$$[C]_{(N+n)\times(N+n)} = \begin{bmatrix}[C_{WT}]_{N\times N} & [0]_{N\times n}\\ [0]_{n\times N} & [0]_{n\times n}\end{bmatrix} + \begin{bmatrix}[C_{WT-WT}]_{N\times N} & [C_{WT-VCS}]_{N\times n}\\ [C_{VCS-WT}]_{n\times N} & [C_{VCS-VCS}]_{n\times n}\end{bmatrix} \quad (3.3)$$

where the submatrices entering Eqs. (3) are expressed with respect to the associated DoFs of the considered VCS. More information regarding the formulation of the submatrices entering Eqs. (3) are provided in the following.

Formulation of TMD submatrices.

The additional mass of the TMD mTMD is attached at the top of the WT tower or inside the nacelle, with a positive stiffness element kTMD and a linear damper cTMD (Fig. 1b). The submatrices can be thus expressed for the TMD VCS as follows:

$$[M_{WT-WT}] = [0]_{24\times24} \tag{4.1}$$

$$[M_{WT-TMD}]^T = [M_{TMD-WT}] = [0]_{1\times24} \tag{4.2}$$

$$M_{TMD-TMD} = m_{TMD} \tag{4.3}$$

$$[K_{WT-WT}] = \begin{bmatrix} 0 & L & 0 \\ M & O & M \\ 0 & L & k_{TMD} \end{bmatrix}_{24\times24} \tag{5.1}$$

$$[K_{WT-TMD}]^T = [K_{TMD-WT}] = [0 \quad L \quad -k_{TMD}]_{1\times24} \tag{5.2}$$

$$K_{TMD-TMD} = k_{TMD} \tag{5.3}$$

$$[C_{WT-WT}] = \begin{bmatrix} 0 & L & 0 \\ M & O & M \\ 0 & L & c_{TMD} \end{bmatrix}_{24\times24} \tag{6.1}$$

$$[C_{WT-TMD}]^T = [C_{TMD-WT}] = [0 \quad L \quad -c_{TMD}]_{1\times24} \tag{6.2}$$

$$C_{TMD-TMD} = c_{TMD} \tag{6.3}$$

Further details regarding the calculation of the TMD parameters k_{TMD} and c_{TMD} will be presented in section 3.

Formulation of EKD submatrices.

With the implementation of the KDamper-based designs (KDamper or EKD), the nacelle is no longer rigidly connected to the top of the WT tower but is mounted on a KDamper-based configuration (Fig. 1b). The procedure for the formulation of the EKD mechanism submatrices will be described in detail from here on, as is the exten-sion of the KDamper. The concentrated mass mNAC is connected to the top of the WT tower with a positive stiffness connection kR, and the additional mass of the EKD mEKD is connected to the mNAC with a negative stiffness element kNS and a linear damper cNS parallel to kNS. In addition, the mEKD is attached to the top of the WT tower with a positive stiffness element kPS and a linear damper cPS parallel to kPS. The submatrices presented in Eqs. (3) are modified in the case where the EKD in employed as follows:

$$[M_{WT-WT}] = \begin{bmatrix} 0 & L & 0 \\ M & O & M \\ 0 & L & -m_{NAC} \end{bmatrix}_{24\times24} \tag{7.1}$$

$$[M_{WT-EKD}]^T = [M_{EKD-WT}] = [0]_{2\times24} \tag{7.2}$$

$$[M_{EKD-EKD}] = \begin{bmatrix} m_{EKD} & 0 \\ 0 & m_{NAC} \end{bmatrix}_{2\times2} \tag{7.3}$$

$$[K_{WT-WT}] = \begin{bmatrix} 0 & L & 0 \\ M & O & M \\ 0 & L & k_R + k_{PS} \end{bmatrix}_{24\times24} \tag{8.1}$$

$$[K_{WT-EKD}]^T = [K_{EKD-WT}] = \begin{bmatrix} 0 & L & -k_{PS} \\ 0 & L & -k_R \end{bmatrix}_{2\times24} \tag{8.2}$$

$$[K_{EKD-EKD}] = \begin{bmatrix} k_{NS} + k_{PS} & -k_{NS} \\ -k_{NS} & k_R + k_{NS} \end{bmatrix}_{2\times2} \tag{8.3}$$

$$[C_{WT-WT}] = \begin{bmatrix} 0 & L & 0 \\ M & O & M \\ 0 & L & c_{PS} \end{bmatrix}_{24\times24} \tag{9.1}$$

$$[C_{WT-EKD}]^T = [C_{EKD-WT}] = \begin{bmatrix} 0 & L & -c_{PS} \\ 0 & L & 0 \end{bmatrix}_{2\times24} \tag{9.2}$$

$$[C_{EKD-EKD}] = \begin{bmatrix} c_{NS} + c_{PS} & -c_{NS} \\ -c_{NS} & c_{NS} \end{bmatrix}_{2\times2} \tag{9.3}$$

Further information for the calculation of the EKD parameters k_R, k_{NS}, k_{PS}, c_{NS} and c_{PS} will be presented in section 3.

3 Constrained Optimization of VCS

Having established the equations of motions of the controlled onshore WT with the investigated VCS, the next objective is to determine the optimal VCS parameters to attain the best possible seismic protection strategy. The design performance of most VCS is strongly dependent on their tuned frequency ratio and damping ratio. Numerous techniques have been proposed for the optimization of the key design parameters of such vibration absorbers. However, the complexity of KDamper-based configurations render the conventional min–max ($H\infty$) approaches ineffective. In this study, the proposed KDamper-based VCS are designed based on engineering criteria and manufacturing as well as geometric limitations and constraints. The parameters of the VCS are evaluated using constrained Optimization Algorithms [28,32], as it is an efficient approach to design effective and practical devices for vibration control. The Harmony Search (HS) algorithm, a novel metaheuristic algorithm is used [46], to determine the optimum values of the independent design parameters of all of the examined VCS. The purpose of the employed VCS is to avoid collapse in case a severe seismic event occurs. Strong earthquakes can be generated from various types of accelerograms, such as synthetic records, real earthquakes excitations and artificial accelerograms, compatible with a specific design response spectrum, with the latter being the most suitable. Further details regarding the excitation input are provided in the following section.

3.1 Seismic Excitation Input

The generation of design response spectrum compatible ground acceleration excitations is necessary, as synthetic records are usually obtained from seismological models and real earthquakes excitations do not cover all soil types and do not have smoothed spectra. The ground motion acceleration excitation input selected in this study is a set of artificial accelerograms designed to be spectrum compatible with the EC8 design acceleration spectrum. More specifically, SeismoArtif software is used for the generation of the database of accelerograms. SeismoArtif computes a power spectral density function from the EC8 acceleration response spectrum and uses this function to derive the amplitudes of sinusoidal signals with random phase angles. The signals are then summed, and an iterative procedure is invoked to improve the match with the target response spectra. The power spectral density function is then adjusted by the square of the ordinate ratio and a new motion is generated. It should be noted that in this research work, only the translational component is accounted for, although the rotational component can also influence the dynamic response of tall structures [47], like WTs.

The target spectrum is the EC8 with characteristics: ground type C, spectral acceleration 0.36 g, spectrum type I, and importance class II. The calculation method used is the Artificial Accelerogram Generation and Adjustment method in the SeismoArtif software. In Fig. 2 a random artificial accelerogram of the database is presented, along with the mean acceleration spectrum of all the accelerograms of the database, compared to the design target spectrum of the EC8 with the aforementioned characteristics. It can be observed that there is a good match in all the range of the presented natural periods.

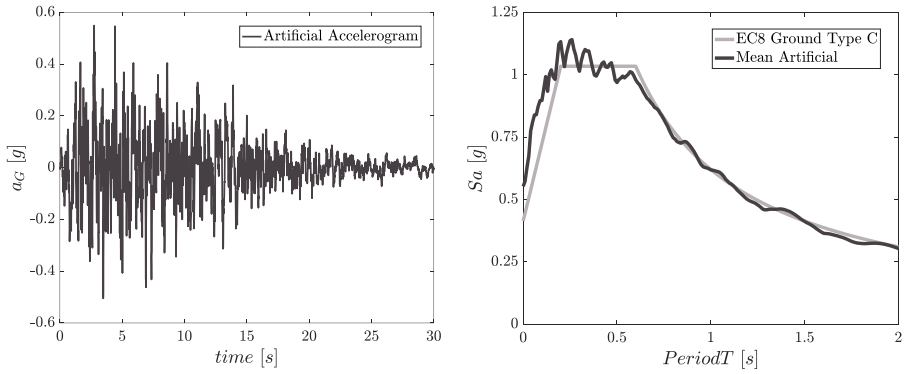

(a) (b)

Fig. 2. (a) Random artificial accelerogram of the database, and (b) mean acceleration spectrum of the artificial accelerograms of the database compared to the EC8 design acceleration spectrum used as the target for the generation of the database

In total 30 artificial accelerograms are generated in the database. The excitation input in the optimization process formulated in this section will be the set of artificial accelerograms, and in section 4 where the optimization results will be presented, the performance of the examined VCS will be also assessed with real earthquake records.

3.2 TMD Optimal Design

The design variables of the TMD configuration installed at the top of the WT tower or inside the nacelle are the mass ratio (μ_{TMD}) of the additional oscillating mass, the tuning TMD frequency ratio (t_{TMD}) and the TMD damping ratio (ζ_{TMD}), that can be expressed with the following relations:

$$\mu_{TMD} = \frac{m_{TMD}}{m_{NAC}} \tag{10.1}$$

$$t_{TMD} = \frac{\omega_{TMD}}{\omega_{(1)}} \tag{10.2}$$

$$\zeta_{TMD} = \frac{c_{TMD}}{2\omega_{TMD} m_{TMD}} \tag{10.3}$$

where m_{NAC} is the added mass at the top of the WT tower to account for the inertial forces applied by the mechanical parts, ω_{TMD} is the TMD frequency and $\omega_{(1)}$ is the fundamental frequency of the primary structure. Common practice is to tune the TMD with the fundamental frequency of the primary structure (t_{TMD} =1), especially in structures where the first eigenfrequency primarily affects the structural dynamic responses, which is usually the case in wind turbine structures. However, in this study in order to have an equal comparison basis with the KDamper-based configurations, the TMD tuning frequency will be a free design variable sought in the optimization procedure, along with its damping ratio ζ_{TMD}. The mass ratio is assumed to be equal to μ_{TMD}=2%, a limit value in such applications, as higher concentrated masses may result in second order phenomena and endanger the structure. Concluding for the design of the TMD, its tuning frequency ratio is selected to vary in the range of 0.75 to 1.25, and the damping ratio is selected to vary in the range of 0% to 30%. A geometric constraint is imposed in the optimization of the TMD regarding the maximum allowed TMD stroke (relative displacement between the TMD and the top of the tower), that is half of the top WT tower diameter 3.87/2≈1.9*m*. Finally, the maximum absolute value of the base shear (mean of max values of the dynamic analyses for all the artificial accelerograms of the database) during the dynamic analysis is set as the objective function in the optimization procedure.

3.3 KDamper-Based Optimal Design

Having established the mass, damping and stiffness matrices of the controlled WT tower with the EKD configuration, the goal now is to optimize its parameters to obtain the best possible seismic protection strategy. The design variables of the EKD are the mass ratio (μ_{EKD}), the tuning frequency of the additional oscillating mass (f_{EKD}), the equivalent stiffness of the nacelle-tower layer ($k_{NAC\text{-}EKD}$), the nominal frequency of the nacelle-tower layer ($f_{NAC\text{-}EKD}$), and the damping ratios of the added linear dampers (ζ_{PS}, ζ_{NS}), and are expressed as follows:

$$\mu_{EKD} = \frac{m_{EKD}}{m_{EKD}} \tag{11.1}$$

$$\omega_{EKD} = 2\pi f_{EKD} = \sqrt{\frac{k_{NS} + k_{PS}}{m_{EKD}}} \tag{11.2}$$

$$k_{NAC-EKD} = k_R + \frac{k_{NS}k_{PS}}{k_{NS} + k_{PS}} \tag{11.3}$$

$$\omega_{NAC-EKD} = 2\pi f_{NAC-EKD} = \sqrt{\frac{k_{NAC-EKD}}{m_{EKD} + m_{NAC}}} \tag{11.4}$$

$$\zeta_{NS,PS} = \frac{c_{NS,PS}}{2\omega_{EKD}m_{EKD}} \tag{11.5}$$

Another critical factor that should be accounted for in case negative stiffness elements are implemented in a vibration control system, such the EKD, is the static and dynamic stability of the controlled WT. To do that, possible variations in all stiffness elements are foreseen in the EKD design process, by introducing simultaneous perturbations ε in all stiffness elements as follows:

$$k_{NAC-EKD}(\varepsilon) = (1 - \varepsilon_R)k_R + \frac{(1 - \varepsilon_{PS})k_{PS}(1 + \varepsilon_{NS})k_{NS}}{(1 - \varepsilon_{PS})k_{PS} + (1 + \varepsilon_{NS})k_{NS}} > 0 \tag{12}$$

Stiffness elements k_R and k_{PS} result from Eqs. (11.4, 12) as a function of the negative stiffness k_{NS} and the nominal frequency of the nacelle-tower layer $f_{NAC\text{-}EKD}$. The additional mass of the EKD is assumed to be significantly lower as compared to the TMD due to the contribution of the negative stiffness to the effective inertia of the added mass and is selected to be equal to μ_{EKD}=0.1%. The stiffness elements variations are assumed in this study as ε_R=ε_{NS}=ε_{PS}=5%. As a result, the free design variables sought in the optimization process of the EKD are:

1. The nominal frequency of the nacelle-tower layer $f_{NAC\text{-}EKD}$ is selected to vary in the range of 0.1*Hz* to 1*Hz*. The same limits are selected for the KDamper system $f_{NAC\text{-}KDamper}$.
2. The value of the negative stiffness element k_{NS}, selected to vary in the range of 0*kN/m* to -100*kN/m* per *tn* of concentrated mass m_{NAC} [48].
3. The value of the linear dampers c_{NS} and c_{PS} selected to vary in the range of 0*kNs/m* to 5*kNs/m* per *tn* of concentrated mass m_{NAC} [48].

The same geometric constraint with the TMD concept is imposed with respect to the stroke of the additional oscillating mass of the EKD, that is the half of the top WT diameter. In addition, another geometric constraint is imposed in the relative displacement between the nacelle and the top of the WT tower for operational reasons [49]: $u_{NAC\text{-}TOW}$=u_{NAC}-u_{TOW}(h=120m)<0.5m. Finally, the maximum absolute value of the base shear (mean of max values of the dynamic analyses for all the artificial accelerograms

of the database) during the dynamic analysis is set as the objective function in the optimization procedure.

4 Optimization Results and Performance Assessment of VCS with Real Earthquakes

Following the optimization process described in section 3 for all considered VCS in this study, the optimized VCS parameters are obtained. The resulting TMD optimal tuning frequency ratio is t_{TMD}=0.827, indicating that higher modes participate when ground motion acceleration excitation is present, revealing that tuning the TMD with the fundamental frequency of the primary structure is not always the optimal solution. The TMD damping ratio resulted in ζ_{TMD}=6%. The TMD managed to reduce the base shear from 4825*kN* to 4607*kN*, a reduction of 4.5%. In addition, with the implementation of the TMD to top WT tower displacement is reduced from 58.3*cm* to 46.5*cm*, a reduction of 20.2%.

The optimal nominal frequency of the nacelle-tower layer with the KDamper system is $f_{NAC\text{-}KDamper}$=0.54*Hz*, the value of the negative stiffness element is k_{NS}=-61.3*kN/m* per *tn* of m_{NAC}, and the value of the artificial damper is c_{PS}=907*kNs/m*. For the EKD configuration, the optimal nominal frequency of the nacelle-tower layer system is $f_{NAC\text{-}EKD}$=0.226*Hz*, the value of the negative stiffness element is k_{NS}=-42.4*kN/m* per *tn* of m_{NAC}, the value of the artificial damper parallel to the NS element is c_{NS}=155*kNs/m*, and the value of the artificial damper parallel to the positive stiffness element is c_{PS}=21*kNs/m*. The KDamper managed to reduce the base shear from 4825*kN* to 2628*kN*, a significant reduction of 45.5%, while the top WT tower displacement is reduced from 58.3*cm* to 24.1*cm*, a reduction of 58.7%. The EKD managed to reduce the base shear from 4825*kN* to 1902*kN*, a reduction of 60.6%, while the top WT tower displacement is reduced from 58.3*cm* to 21.5*cm*, a reduction of 63.1%.

From the optimization results, it is evident that the KDamper-based designs outperform the TMD having significantly lower added mass. The EKD is superior to the KDamper, as it requires lower NS and damping values. In Fig. 3, the dynamic responses of the primary WT, and the WT equipped with a TMD and an EKD are presented.

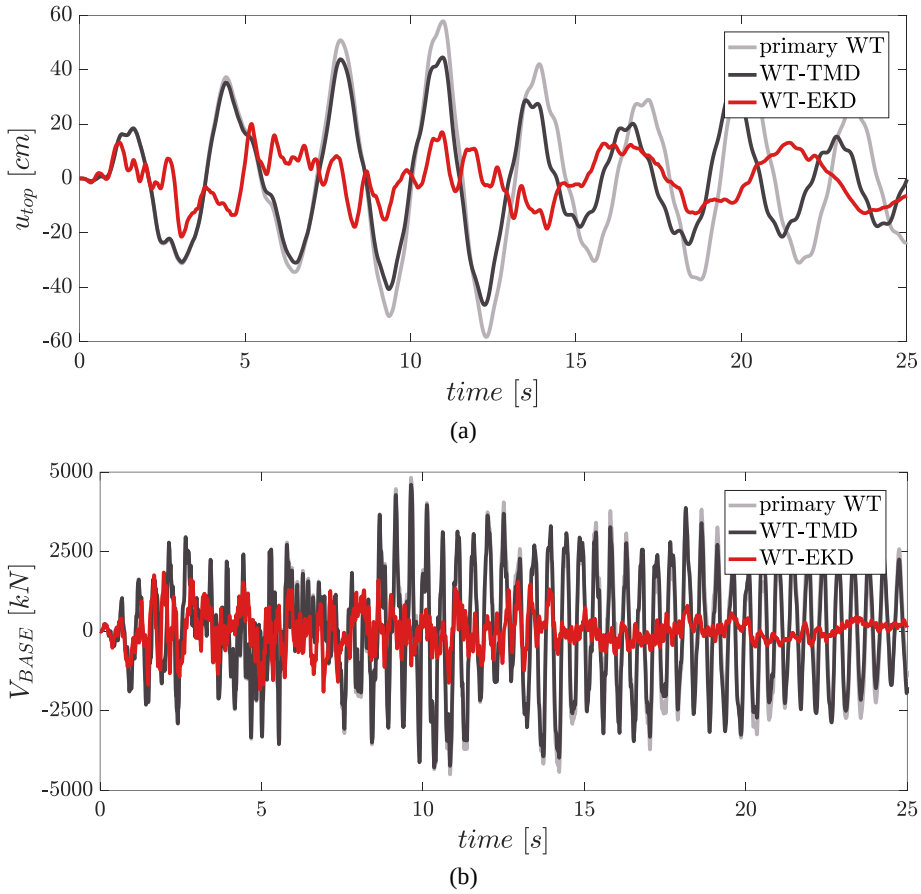

Fig. 3. Dynamic responses of the primary WT, and the WT equipped with a TMD and an EKD for a random artificial accelerogram of the database. (a) Top WT relative to the ground displacement and (b) base shear

Aiming to validate the effectiveness of the investigated VCS as seismic protection strategies and examine their dynamic performance, an ensemble of 8 recorded real ground motions is adopted as input ground motion acceleration excitation to the benchmark WT. The selected records cover a wide range and variety of key seismic characteristics such as peak ground acceleration (PGA) and magnitude (Mw), as well as broad frequency content, duration, and number of significant acceleration cycles. The characteristics of the selected seismic excitations are provided in Table 1. These records have large magnitudes Mw ranging from six to eight, and they are categorized as Near-Fault (NF) due to their Joyner-Boore distance R_{jb} being less than $25km$. Their PGA is on average equal to PGA = 0.35 g. The significant duration of the records, denoted as $Dur_{5-75\%}$, is defined as the time needed to build up between 5% and 75% of the total Arias intensity.

Table 1. Seismic characteristics of the selected real earthquake records

No	Earthquake	Year	Station	Ground Motion	Mw	PGA (g)	PGA/PGV (gsec/m)	R_{JB} (km)	$Dur_{5\text{-}75\%}$ (sec)
1	Northridge	1994	N Hollywood	Near fault	6.69	0.3087	1.4389	7.89	7.0
2	L'Aquila	2009	V. Aterno	Near fault	6.3	0.4018	1.2548	0.0	4.7
3	Kocaeli	1999	Izmit	Near fault	7.51	0.1651	0.7396	3.62	8.2
4	Tabas	1978	Tabas	Near fault	7.35	0.8540	0.8639	1.79	8.3
5	Kobe	1995	Amagasaki	Near fault	6.9	0.2758	0.8214	11.34	6.9
6	Landers	1992	Joshua tree	Near fault	7.28	0.2736	1.0125	11.03	21.7
7	Duzce	1999	Lamont 1059	Near fault	7.14	0.1524	1.1844	4.17	10.4
8	Friuli	1976	Tolmezzo	Near fault	6.5	0.3571	1.5629	14.97	2.5

Time-history analyses are subsequently performed for all the selected real earthquake records and VCS configurations. In Fig. 4, the maximum absolute values of the WT tower top displacement (Fig. 4a) and the maximum absolute values of the base shear (Fig. 4b) are presented, expressed as a percentage of the respective values of the dynamic responses of the primary uncontrolled WT.

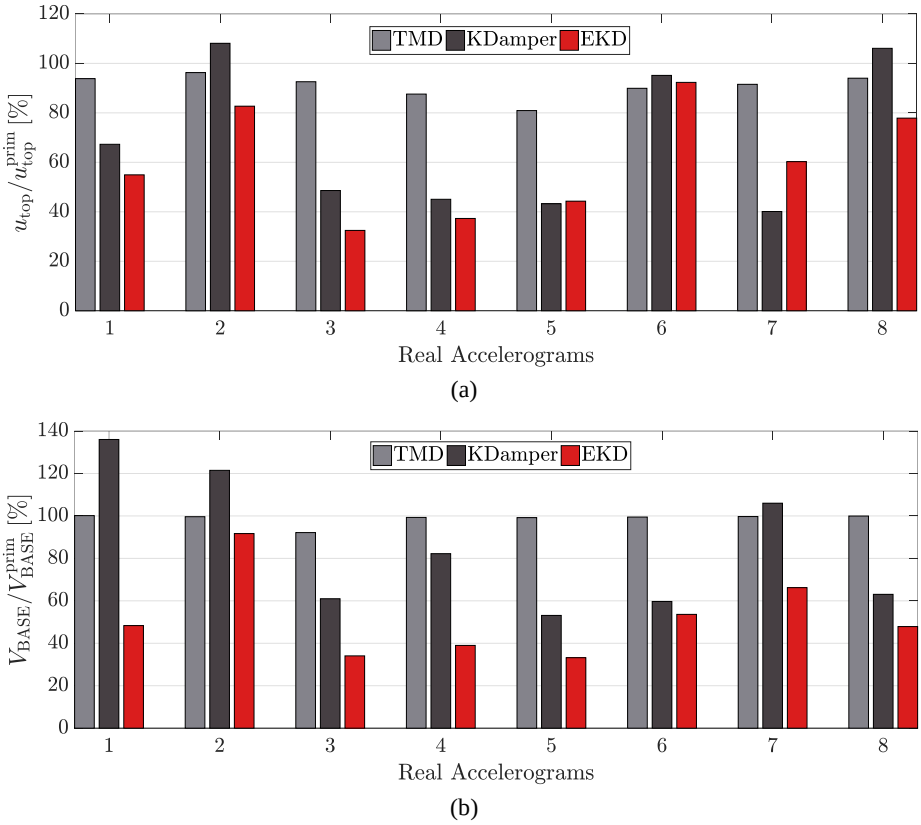

Fig. 4. Comparative dynamic analyses results (expressed as a percentage of the respective values of the primary uncontrolled WT) among the controlled WT with a TMD, a KDamper, and an EKD for all the selected real ground motions. (a) Top WT relative to the ground displacement and (b) base shear

It is observed that the EKD is consistent in significantly reducing the WT dynamic responses, while the KDamper in some cases amplifies the WT top displacement (in 2 out of 8 records) and the base shear (in 3 out of 8 records). On the other hand, the TMD slightly improves the base shear of the WT in the order of 2-3% on average and has a consistent performance with respect to the WT top tower displacements, however, not as much as the EKD configuration. Finally, in Fig. 5 the dynamic responses of the primary WT, and the WT equipped with a TMD and an EKD are presented for the Kocaeli record (No. 3 in Table 1).

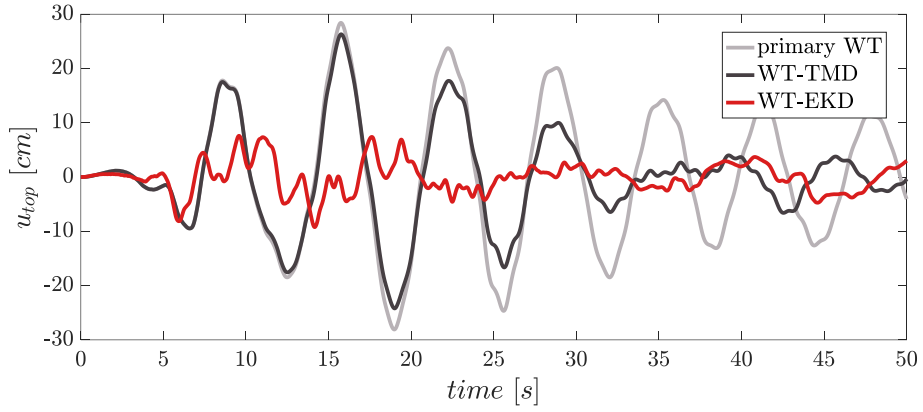

(a)

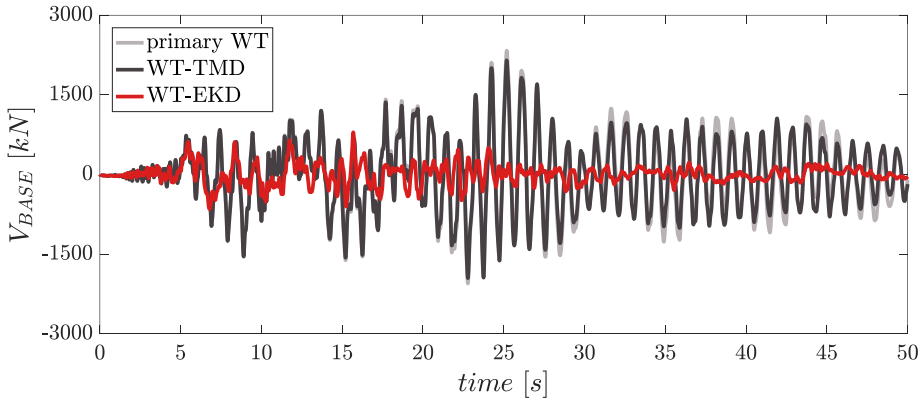

(b)

Fig. 5. Dynamic responses of the primary WT, and the WT equipped with a TMD and an EKD for Kocaeli (1999) earthquake record (No. 3 of Table 1). (a) Top WT relative to the ground displacement and (b) base shear

5 Conclusions

In this paper, the use of KDamper-based configurations is proposed for the seismic protection of an onshore wind turbine. The dynamic model of the WT tower is an assemblage of prismatic beam elements, and for the numerical modelling of the proposed formulation a built-in house soft-ware is developed in MATLAB code employing the New-mark-β method for the dynamic analysis. A constrained optimization methodology is formulated for the design of the VCS, that employes engineering criteria and manufacturing and geometrical limitations and constraints. The excitation input is based on the provisions of the EC8 by generating a database of EC8 spectrum compatible database of artificial accelerograms. An extensive case study is carried out

providing insight into the WT structural dynamics. The main conclusions that can be drawn from this research work are the following:

i. The developed dynamic model of the WT tower is serviceable due to the fact that it can easily incorporate each considered VCS for seismic protection, facilitating the optimization procedure.
ii. The KDamper-based designs are not dependent on the additional introduced mass, contrary to traditional mass-related vibration absorbers such as the TMD, as in this study the TMD is designed with an additional mass of 2%, while KDamper-based VCS have 0.1%.
iii. The TMD manages to reduce (mean reduction values for all the artificial accelerograms) the WT base shear by 4.5% and the top WT tower displacement by 20.2%. The KDamper manages to reduce the base shear by 45.5%, while the top WT tower displacement is reduced by 58.7%. The EKD reduces the base shear by 60.6%, and the top WT tower displacement by 63.1%.
iv. The extension of the KDamper concept, i.e. the EKD, is a robust solution, with consistent performance for all of the real earthquake records examined. In addition, the EKD does not require high damping values or even high negative stiffness values.

Building on the findings of this study, future research could incorporate a detailed finite element model (FEM) analysis to evaluate potential local failures, particularly at critical junctions such as the nacelle-tower connection, under seismic and operational loads. Additionally, further studies could investigate the impact of wind turbine operation, specifically the rotational effects of the blades, on the WT seismic response characteristics, providing a more comprehensive understanding of the dynamic behavior of the controlled WT with the proposed KDamper-based devices under real-world conditions.

References

1. Chou Jui-Sheng, Tu Wan-Ting: Failure analysis and risk management of a collapsed large wind turbine tower. Engineering Failure Analysis 18(1), 295–313 (2011). DOI: https://doi.org/10.1016/j.engfailanal.2010.09.008
2. Yao Li, Caichao Zhu, Chaosheng Song, Jianjun Tan: Research and development of the wind turbine reliability. International Journal of Mechanical Engineering and Applications 6(2), 35-45 (2018). DOI: https://doi.org/10.11648/j.ijmea.20180602.14
3. Murtagh, P. J., Ghosh, A., Basu, B., Broderick, B. M.: Passive control of wind turbine vibrations including blade/tower interaction and rotationally sampled turbulence. Wind Energy 11(4), 305–317 (2008). DOI: https://doi.org/10.1002/we.249
4. Lackner, M. A., Rotea, M. A.: Passive structural control of offshore wind turbines. Wind Energy 14(3), 373–388 (2011). DOI: https://doi.org/10.1002/we.426
5. Stewart, G. M., Lackner, M. A.: The impact of passive tuned mass dampers and wind–wave misalignment on offshore wind turbine loads. Engineering Structures 73, 54-61 (2014). DOI: https://doi.org/10.1016/j.engstruct.2014.04.045
6. Avila, S., Shzu, M., Morais, M., Prado, Z.: Numerical modeling of the dynamic behavior of a wind turbine tower. Advances in Vibration Engineering 4 (2016)

7. Zhang Zili, Nielsen Søren, Blaabjerg Frede, Zhou Dao.: Dynamics and control of lateral tower vibrations in offshore wind turbines by means of active generator torque. Energies 7(11), 7746–7772 (2014). DOI: https://doi.org/10.3390/en7117746
8. Maldonado, V., Boucher, M., Ostman, R., Amitay, M.: Active Vibration Control of a Wind Turbine Blade Using Synthetic Jets. International Journal of Flow Control 1(4), 227-238 (2009). DOI: https://doi.org/10.1260/1756-8250.1.4.227
9. Ricciardelli, F., Pizzimenti, A. D., Mattei, M.: Passive and active mass damper control of the response of tall buildings to wind gustiness. Engineering Structures 25(9), 1199–1209 (2003). DOI: https://doi.org/10.1016/S0141-0296(03)00068-3
10. Casciati, F., Rodellar, J., Yildirim, U.: Active and semi-active control of structures – theory and applications: A review of recent advances. Journal of Intelligent Material Systems and Structures 23(11), 1181–1195 (2012) DOI:https://doi.org/10.1177/1045389X12445029
11. Weber F.: Optimal semi-active vibration absorber for harmonic excitation based on controlled semi-active damper. Smart Materials and Structures 23(9) (2014) DOI: https://dx.doi.org/10.1088/0964-1726/23/9/095033
12. Pnevmatikos, N.: New strategy for controlling structures collapse against earthquakes. Natural Science 4(8A), 667-676 (2012)
13. Soong, T. T., Dargush, G. F.: Passive energy dissipation systems in structural engineering. Wiley (1997)
14. Casciati, F., Giuliano, F.: Performance of multi-TMD in the towers of suspension bridges. Journal of Vibration and Control 15(6), 821–847 (2009) DOI: https://doi.org/10.1177/1077546308091455
15. Nigdeli, S. M., Bekdaş, G.: Optimum tuned mass damper design in frequency domain for structures. KSCE Journal of Civil Engineering, 21(3), 912–922 (2017) DOI: https://doi.org/10.1007/s12205-016-0829-2
16. Zuo, H., Bi, K., Hao, H.: Using multiple tuned mass dampers to control offshore wind turbine vibrations under multiple hazards, Engineering Structures 141, 303–315 (2017). DOI: https://doi.org/10.1016/j.engstruct.2017.03.006
17. Chapain S., Aly, A. M.: Vibration attenuation in wind turbines: A proposed robust pendulum pounding TMD. Engineering Structures, 233 (2021) DOI: https://doi.org/10.1016/j.engstruct.2021.111891
18. García, V., J., Duque, E. P., Inaudi, J., A., Márquez, C., O., Mera, J., D., Rios A., C.: Pendulum tuned mass damper: optimization and performance assessment in structures with elastoplastic behavior. Heliyon 7(6) (2021). DOI: https://doi.org/10.1016/j.heliyon.2021.e07221
19. Xue, S. D., Ko, J.M., Xu, Y.L.: Tuned liquid column damper for suppressing pitching motion of structures. Engineering Structures 22(11), 1538-1551 (2000) DOI: https://doi.org/10.1016/S0141-0296(99)00099-1
20. Basu, B., Colwell, S.: Vibration control of an offshore wind turbine with a tuned liquid column damper. In: 11th International Conference on Civil, Structural and Environmental Engineering (2007)
21. Colwell, S., Basu, B.: Tuned liquid column dampers in offshore wind turbines for structural control. Engineering Structures 31(2), 358-368 (2009) DOI: https://doi.org/10.1016/j.engstruct.2008.09.001
22. Zhang, Z. L., Chen, J. B., Li, J.: Theoretical study and experimental verification of vibration control of offshore wind turbines by a ball vibration absorber. Structure and Infrastructure Engineering, 10(8), 1087–1100 (2013) DOI: https://doi.org/10.1080/15732479.2013.792098

23. Chen, J., Georgakis, C. T.: Tuned rolling-ball dampers for vibration control in wind turbines. Journal of Sound and Vibration 332(21), 5271-5282 (2013) DOI: https://doi.org/10.1016/j.jsv.2013.05.019
24. Chen, J.-L., Georgakis, C. T.: Spherical tuned liquid damper for vibration control in wind turbines. Journal of Vibration and Control 21(10), 1875-1885 (2015) DOI: https://doi.org/10.1177/1077546313495911
25. Weber, B., Feltrin, G.: Assessment of long-term behavior of tuned mass dampers by system identification. Engineering Structures 32(11), 3670–3682 (2010) DOI: https://doi.org/10.1016/j.engstruct.2010.08.011
26. Antoniadis, I. A., Kanarachos, S. A., Gryllias, K., Sapountzakis, I. E.: KDamping: A stiffness based vibration absorption concept. Journal of Vibration and Control 24(3), 588–606 (2018). DOI: https://doi.org/10.1177/1077546316646514
27. Carrella, A., Brennan, M. J., Waters, T. P.: Static analysis of a passive vibration isolator with quasi-zero-stiffness characteristic. Journal of Sound and Vibration 301(3-5), 678–689 (2007). DOI: https://doi.org/10.1016/j.jsv.2006.10.011
28. Kapasakalis, K. A., Antoniadis, I. A., Sapountzakis, E. J.: Constrained optimal design of seismic base absorbers based on an extended KDamper concept. Engineering Structures 226 (2021). DOI: https://doi.org/10.1016/j.engstruct.2020.111312
29. Kapasakalis, K. A., Antoniadis, I. A., Sapountzakis, E. J.: Feasibility Assessment of Stiff Seismic Base Absorbers. Journal of Vibration Engineering & Technologies, 10, 37–53 (2021) DOI: https://doi.org/10.1007/s42417-021-00362-2
30. Sapountzakis, E., Florakis, G., Kapasakalis, K.: Design and performance assessment of base isolated structures supplemented with vibration control systems. Buildings 14(4) (2024). DOI: https://doi.org/10.3390/buildings14040955
31. Smith, M. C.: Synthesis of Mechanical Networks: The Inerter. IEEE Transactions on Automatic Control 47(10), 1648-1662 (2002). DOI: 10.1109/TAC.2002.803532
32. Florakis, G. I., Kapasakalis, K. A., Sapountzakis, E. J.: Simplified design approach of a negative stiffness-based seismic base absorber via multi-objective optimization. Soil Dynamics and Earthquake Engineering 189 (2025) DOI: https://doi.org/10.1016/j.soildyn.2024.109092
33. Florakis, G. I., Kapasakalis, K. A., Sapountzakis, E. J.: Frequency-domain optimization of seismically isolated structures enhanced with negative stiffness devices. Mechanical Systems and Signal Processing 228 (2025) DOI: https://doi.org/10.1016/j.ymssp.2025.112375
34. Florakis, G. I., Kapasakalis, K. A., Antoniadis, I. A., Sapountzakis, E. J.: Dimensioning and realistic design of a novel based negative stiffness seismic isolator. Journal of Physics: Conference Series 2647(25) (2024) DOI: https://doi.org/10.1088/1742-6596/2647/25/252020
35. Mantakas, A., Kalderon, M., Chondrogiannis, K. A., Kapasakalis, K. A., Chatzi, E., Antoniadis, I. A., Sapountzakis, E. J.: Experimental testing and numerical validation of the extended kdamper: A negative stiffness-based vibration absorber. Engineering Structures 321 (2024). DOI: https://doi.org/10.1016/j.engstruct.2024.118894
36. Florakis, G. I., Antoniadis, I. A., Sapountzakis, E. J.: A novel gas spring based negative stiffness mechanism for seismic protection of structures. Engineering Structures 291 (2023). DOI: https://doi.org/10.1016/j.engstruct.2023.116389
37. Kapasakalis, K. A., Florakis, G. I., Antoniadis I. A., Sapountzakis, E. J.: Seismic protection of multi-story structures with novel vibration absorption devices combining negative stiffness and inerter. In: 8th International Conference on Computational Methods in

Structural Dynamics and Earthquake Engineering, pp. 4026–4045, Athens, Greece (2021). DOI: https://doi.org/10.7712/120121.8765.19225
38. Mantakas, A. G., Kapasakalis K. A., Alvertos, A. E., Antoniadis, I. A., Sapountzakis, E. J.: A negative stiffness dynamic base absorber for seismic retrofitting of residential buildings. Structural Control and Health Monitoring 29(12) (2022) DOI: https://doi.org/10.1002/stc.3127
39. Kapasakalis K., Mantakas A., Kalderon M., Antoniou, M., Sapountzakis, E.: Performance evaluation of distributed extended kdamper devices for seismic protection of mid-rise building structures. Journal of Earthquake Engineering 28 (4), 972-997 (2023). DOI: https://doi.org/10.1080/13632469.2023.2226227
40. Kapasakalis, K. A., Antoniadis, I. A., Sapountzakis, E. J.: Stiff vertical seismic absorbers. Journal of Vibration and Control 28 (15-16), 1937–1949 (2022) DOI: https://doi.org/10.1177/10775463211001624
41. Gkikakis, A. E., Kapasakalis, K. A., Sapountzakis E. J.: Comprehensive design optimization of vertical seismic absorbers incorporating sensitivity and robust analysis: A case study of the kdamper. Engineering Structures 301 (2024). DOI: https://doi.org/10.1016/j.engstruct.2023.117303.
42. Sapountzakis, E. J., Syrimi, P. G., Pantazis, I. A., Antoniadis, I. A.: KDamper concept in seismic isolation of bridges with flexible piers. Engineering Structures 153, 525–539 (2017). DOI: https://doi.org/10.1016/j.engstruct.2017.10.044.
43. Kapasakalis, K., Gkikakis, A., Sapountzakis, E., Chatzi, E., Kampitsis, A.: Multi-objective optimization of a negative stiffness vibration control system for offshore wind turbines. Ocean Engineering 303 (2024) DOI: https://doi.org/10.1016/j.oceaneng.2024.117631
44. Kampitsis, A., Kapasakalis, K., Via-Estrem, L.: An integrated FEA-CFD simulation of offshore wind turbines with vibration control systems. Engineering Structures 254 (2022). DOI: https://doi.org/10.1016/j.engstruct.2022.113859
45. Quilligan, A., O'Connor, A., Pakrashi, V.: Fragility analysis of steel and concrete wind turbine towers. Engineering Structures 36, 270–82 (2012)
46. Geem, Z.W., Kim, J.H., Loganathan, GV.: A new heuristic optimization algorithm: Harmony search. Simulation 76(2), 60–8 (2001)
47. Pnevmatikos, N., Konstandakopoulou, F., Papagiannopoulos, G., Hatzigeorgiou, G., Papavasileiou, G.: Influence of Earthquake Rotational Components on the Seismic Safety of Steel Structures. Vibration 3(1), 42-50 (2020)
48. Kapasakalis, K.: Dynamic Vibration Absorbers in Civil Engineering Structures, Doctoral Dissertation, National Technical University of Athens (2020)
49. Kapasakalis, K., Antoniadis, I., Sapountzakis, E., Kampitsis, A.: Vibration Mitigation of Wind Turbine Towers Using Negative Stiffness Absorbers. Journal of Civil Engineering and Construction 10(3), 123-139 (2021)